

Deep-Learning-Based Onset Time Precision in Acoustic Emission Non-Destructive Testing

Original

Deep-Learning-Based Onset Time Precision in Acoustic Emission Non-Destructive Testing / Melchiorre, J.; D'Amato, L.; Agostini, F.; Manuello, A.. - 2004:(2024), pp. 367-372. (Intervento presentato al convegno 2024 IEEE International Workshop on Metrology for Living Environment, MetroLivEnv 2024 tenutosi a Chania (GRC) nel 12-14 June 2024) [10.1109/MetroLivEnv60384.2024.10615695].

Availability:

This version is available at: 11583/2991916 since: 2024-08-24T16:17:15Z

Publisher:

Institute of Electrical and Electronics Engineers Inc.

Published

DOI:10.1109/MetroLivEnv60384.2024.10615695

Terms of use:

This article is made available under terms and conditions as specified in the corresponding bibliographic description in the repository

Publisher copyright

IEEE postprint/Author's Accepted Manuscript

©2024 IEEE. Personal use of this material is permitted. Permission from IEEE must be obtained for all other uses, in any current or future media, including reprinting/republishing this material for advertising or promotional purposes, creating new collecting works, for resale or lists, or reuse of any copyrighted component of this work in other works.

(Article begins on next page)

Deep-learning-based onset time precision in acoustic emission non-destructive testing

Jonathan Melchiorre*, Leo D'Amato[†], Federico Agostini[‡], and Amedeo Manuello*

*Department of Structural, Geotechnical and Building Engineering, Politecnico di Torino, Turin, Italy.

Email: jonathan.melchiorre@polito.it, amedeo.manuello@polito.it

[†]Politecnico di Torino, DAUIN, Department of Control and Computer Engineering,

Corso Castellidardo, 34/d, Turin, Italy.

Email: leo.damato@polito.it

[‡]University of Padua, Department of Physics and Astronomy, Padua, Italy.

Abstract—To investigate the actual health status and mechanical properties of structural materials, both direct and/or indirect investigation procedures can be used. The acoustic emission (AE) method is a non-destructive indirect structural health monitoring method based on the analysis of the elastic wave propagation inside the material under study induced during cracks and micro-cracks coalescence, opening, and formation process. To capture reliable ultrasonic elastic waveform data, piezoelectric sensors are typically employed which are directly and firmly fixed and attached to the specimen under study. For identifying the region of crack formation, thus the position of structural damage in its early stage, at least four sensors must be employed simultaneously. Furthermore, the identification of the onset time is crucial to accomplishing this task. In this study, the authors proposed a deep-learning-based solution based on a U-net architecture for identifying onset time with a method attempting to overcome the existing limitations of traditional threshold-based methods. The onset time precision obtained with this artificial intelligence-based (AI) paradigm is discussed on an acknowledged dataset available in the literature based on Pencil Lead Break (PLB) data, commonly used as a benchmark in the AE field. Finally, the method is tested on some real AE signals acquired during laboratory testing of reinforced concrete specimens. The results demonstrated the actual potential of the proposed AI-based method in future real-time monitoring real-world applications.

I. INTRODUCTION

The recent advancements in artificial intelligence (AI) [1], particularly deep learning, have revolutionised engineering by providing innovative solutions and insights [2]. Deep learning, inspired by the human brain [3], excels at automatically learning complex patterns from data, making it a versatile tool for solving various engineering problems. This paper explores the application of deep learning in detecting the onset time in Acoustic Emission (AE) signals. Acoustic Emission (AE) is a non-destructive technique [4] widely used in Structural Health Monitoring (SHM) [5] to monitor historical buildings [6] and structures [7]. It allows the understanding of structural dynamics and enables prompt interventions to extend the service life of structures. AE stands out in SHM due to its passive nature [8], being not necessary to physically damage or excite the structures. Transient ultrasonic waves are recorded by piezoelectric sensors [9]. These waves are produced when the accumulated elastic energy in cracks is

released. These waves are converted into an electric voltage by the sensors, which can then be digitised and analysed [10]. The study of collected signals provide insight into the genesis and progression of cracking patterns. Based on the analysis of AE signals, a variety of methodologies have been developed to localize, characterize, and quantify damage. The primary applications of Acoustic Emission (AE) technology are the localization of cracks and their categorization. This study focuses on the latter, which is of crucial importance for the understanding of damage causes and the facilitation of timely maintenance. Precise localization of damage depends critically on the onset time of an AE signal, which is the instant the elastic wave encounters the piezoelectric sensors. Over the years, numerous strategies for automatically detecting the onset time have been developed [11], [12], [13]. In order to address these issues, recent years have seen the emergence of novel methodologies that employ artificial intelligence (AI) and machine learning (ML) techniques [14], [15]. Machine learning and deep learning algorithms have shown effective in precisely predicting the onset time of acoustic emission signals [16], [17]. Nevertheless, current methodologies still exhibit limitations, including computational and storage intensity or the necessity for data preprocessing techniques to enhance Signal-to-Noise Ratio (SNR) [18]. Furthermore, these techniques frequently necessitate signal segmentation, thereby requiring additional preprocessing for classification [19]. This research presents a novel deep learning model that uses a U-Net neural network [20] to detect the onset times of acoustic emission sources. The model reduces the onset time detection problem to an a single-dimensional segmentation task, identifying each point in the data as either signal or background noise. A rolling average probability is used to reduce false positives by smoothing the probability curve over time. The proposed architecture is optimised for accuracy, computational efficiency, and storage, resulting in a lighter model compared to traditional convolutional neural networks. Furthermore, the approach is designed to operate directly on continuous signals, eliminating the requirement for preprocessing. The goal is to develop a technique that can be used to identify onset times in real time on the field. The models are trained using data collected through a Pencil Lead Break test (PLB) [21]. The

rationale behind this approach is to simulate the AE signal by fracturing a pencil lead against a concrete block. Since the position of the pencil lead is known, this test enables the recording of labelled signals in which the onset time is known. In general, this type of test is widely used for the calibration of the recording instrumentation. Following the training on the PLB dataset, the method is qualitatively evaluated on a real-world dataset of authentic acoustic emissions, without any finetuning. The real data has been recorded during a three-point bending test conducted on a beam made of FRC (fiber-reinforced concrete).

II. METHODOLOGY

Identifying the onset time in Acoustic Emission (AE) signals is crucial for crack localization. In a simplified model, it is possible to precisely localize crack through AE signal onset times using at least 5 sensors [22]. In such model, the shortest wave path is assumed, as P-wave onset times are less affected by disturbances and are used for crack localization. The distance d_{0-A} between the crack source $S_0 = (x_0, y_0, z_0)$ and sensor $S_A = (x_A, y_A, z_A)$ is calculated using:

$$d_{0-A} = \sqrt{(x_0 - x_A)^2 + (y_0 - y_A)^2 + (z_0 - z_A)^2}$$

Assuming a homogeneous medium with constant wave speed c , the travel time T_A is:

$$T_A = \frac{d_{0-A}}{c}$$

The unknowns (x_0, y_0, z_0) , crack event time t_0 , and wave speed c prevent direct solution. However, relative arrival times Δt_A at each sensor can be analyzed, leading to:

$$\begin{aligned} \Delta t_A &= T_A - T_R \\ &= \frac{\sqrt{(x_0 - x_A)^2 + (y_0 - y_A)^2 + (z_0 - z_A)^2}}{c} - T_R \end{aligned}$$

Hence, with at least 5 sensors, it is possible to precisely localize the crack through AE signal onset times.

While experts can manually identify onset times, automatic identification is needed for real-time monitoring, especially given the large volume of recorded signals. Various methods for onset time identification exist, including machine learning approaches.

In this paper a deep learning-based method using a U-Net architecture [20] for onset time identification is introduced. U-Net, a type of Convolutional Neural Network (CNN), is designed for segmentation tasks and is effective in various applications. U-Net is an encoder-decoder model that captures local and global context information. The encoder uses convolutional and pooling operations to reduce spatial dimensions and extract high-level features. It consists of multiple blocks with convolutional layers followed by ReLU activation and max-pooling layers. The decoder restores spatial information through up-convolutional and concatenation operations, creating a segmentation map matching the input

matrix dimensions. The decoder blocks, which include up-convolutional layers, enhance spatial resolution and merge features from the encoder through skip connections, which improve segmentation accuracy. In this study, we evaluate the efficacy of different U-Net models obtained by varying the number of convolutional blocks. The simplest models includes only one convolutional block, while the more complex models include four convolutional blocks. Each block has two one-dimensional convolutional layers with GELU activation. The decoder is intended to duplicate the encoder, with the added functionality of upsampling for temporal resolution. The final output layer, a one-dimensional convolutional layer with softmax function activation, generates a pixel-wise probability map indicating the likelihood of each point being a signal or background noise. The U-Net architecture is remarkable for its use of skip connections, which connect map features from the contracting path to equivalent blocks on the expansion path. This approach enables the decoder to acquire and use multi-scale data from previous network stages, boosting the precision of segmentation. A pixel-wise probability map is generated at the conclusion of the expanded path using a 1x1 convolutional layer with softmax activation. The result map shows the likelihood of each pixel falling into a particular class. The network is tuned during training with appropriate loss functions, including cross-entropy loss or dice loss, to minimize the discrepancy between the segmentation maps predicted and the ground truth. To summarize, the U-Net design offers a strong framework for segmentation tasks, exploiting both global and local context information via its encoder-decoder architecture and skip connections. The approach in this study involves the use time series as input to the deep learning model, eliminating the need for Fourier transform pre-processing. This method significantly reduces the computational cost compared to approaches using 2D or 3D input data. For every signal point, the model returns a probability indicating whether it is part of the AE signal or background noise. A probability threshold is defined, and points with probabilities greater than this threshold are categorized as part of the AE signal.

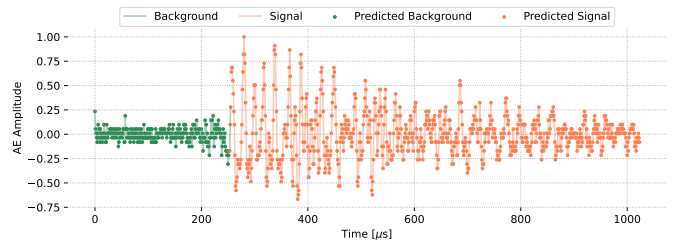


Fig. 1. Example of signal segmentation in "background" or "signal" achieved by utilizing a U-Net model.

The neural model segments the one-dimensional signal to classify each point into two classes: background noise and AE signal. It assigns each point a probability of belonging to either class, which helps to identify the onset time. An example of signal classification is shown in Figure 1. The onset time is defined as the point at which the background

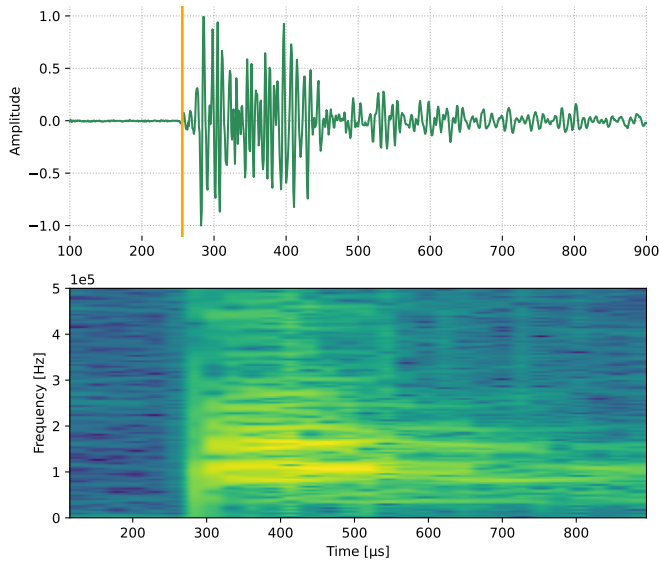


Fig. 2. AE signal depicted in both a time-series (top) and a spectrogram (bottom). The frequencies are reported in Hertz [Hz] and the amplitudes are normalised.

noise transitions to the AE signal. The U-Net neural network was trained using data from [21]. This dataset is derived from artificial acoustic emission (AE) tests performed on a block of concrete using pencil lead breaks (PLBs) to generate elastic waves. The dataset comprises 98 time-series of acoustic emission (AE) signals recorded from laboratory experiments on concrete samples. These signals, sampled at 10,000 kHz, are represented as both time-series and spectrograms in Figure 2. However, distinguishing between background noise and the AE signal in the spectrograms is challenging due to similar frequencies, especially in concrete structures.

Each AE signal has 1024 time samples and a continuous pre-triggering duration of $256\mu s$ before the onset time event. The labels are as follows: label 0 corresponds to background noise and label 1 to the AE signal. The objective of this study is to automate onset time identification in AE signals for real-time applications. For this purpose, the dataset is processed in such a way that it contains non-uniformly spaced AE signals. This is achieved by concatenating the time-series into one long signal and segmenting it into windows with varying lengths. Additionally, random segments are trimmed from the initial part of each signal containing background noise. Subsequently, the aforementioned processed dataset is divided into a 75% training set and a 25% validation set for the purposes of model training and evaluation, respectively. In this work, the input sequence length and U-Net architectural depth are varied to assess the effectiveness of several neural models. Three depths (2, 3, and 4) and three input sequence lengths (512, 1024, and 2048 samples) are compared. For training, the maximum number of epochs is set to 200 to balance computational efficiency and model convergence, with early stopping implemented to prevent overfitting. Due to its applicability in binary classification problems, binary cross-

entropy is adopted as the loss function. The learning rate of the ADAM optimiser is set to 10^{-4} to facilitate faster convergence and enhanced performance. These choices are made with the objective of optimising the training process and ensuring effective learning of data patterns. Following the training process, classification errors are analyzed. It is observed that model errors consist of samples from background noise incorrectly classified as part of the AE signal, while the model rarely misclassify samples from the signal as background noise. These misclassifications lead the signal to have false onset times. Table I presents a summary of the number of erroneous onset timings obtained by the various models, including both the training and validation sets.

| Model Seq. Len. | Depth | U-Net Predictions | | R.A. Correction | |
|-----------------|-------|-------------------|------------|-----------------|------------|
| | | Train | Validation | Train | Validation |
| 2048 | 4 | 0 | 19 | 0 | 1 |
| 2048 | 3 | 0 | 57 | 0 | 10 |
| 2048 | 2 | 191 | 242 | 9 | 13 |
| 1024 | 4 | 0 | 21 | 0 | 2 |
| 1024 | 3 | 0 | 56 | 0 | 7 |
| 1024 | 2 | 485 | 270 | 32 | 24 |
| 512 | 4 | 5 | 22 | 2 | 2 |
| 512 | 3 | 0 | 70 | 0 | 5 |
| 512 | 2 | 625 | 282 | 37 | 21 |

TABLE I
THE NUMBER OF ERRONEOUS ONSET TIMES FOUND BY U-NET OUTPUTS BEFORE AND AFTER USING THE ROLLING AVERAGE ADJUSTMENT.

In order to reduce the classification errors, a smoothing technique is applied to the probability values derived from the U-Net output. Figure 3 illustrates how these errors frequently result in localized variations in the probability values. In order to achieve a smoother probability function derived from the U-Net output, it is necessary to average the probability values over a window of fifty samples.

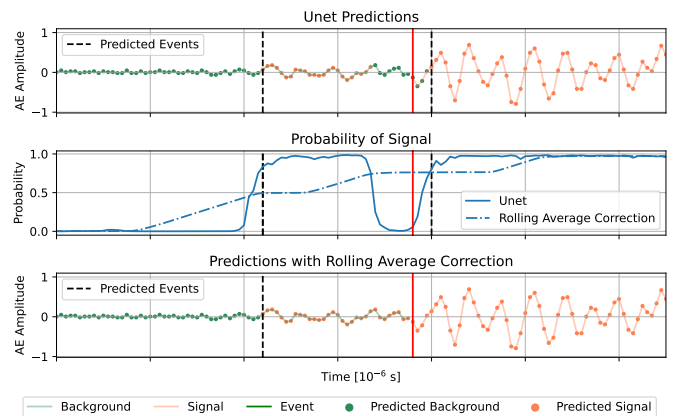


Fig. 3. The impact of smoothed probability with rolling average correction. The top graph shows predictions based on model output probabilities. The graph in the middle compares U-Net probability to the rolling average correction. The bottom graph displays forecasts based on smoothed probability.

This approach significantly reduces the occurrence of spurious onset times. Table I compares the number of false onset times obtained with direct classification against corrected classification using the rolling average approach. The approach

was highly effective, lowering false onset times by over 90% in several cases.

The evaluation metrics of the various neural models for both the validation and training sets are presented in Table II. The table presents the outcomes of varying the input sequence length and the U-Net architecture depth, which ranges from two to four layers. Extending the input sequence is a way to capture more context surrounding the event and enhancing the model capability to correctly identify the onset time. An increase in the number of levels and parameters in the ANN results in a more accurate fit to the dataset while avoiding overfitting.

The metrics presented in Table II demonstrate the efficacy of the models in identifying signal samples and distinguishing between background noise and AE signals. The models achieve accuracies exceeding 0.97, with some exceeding 0.9999. The mean absolute error (MAE) values are notably low, with the optimal result of 0.006 observed on the test set. However, these metrics evaluate the categorisation of individual samples within a time series, where the initial background noise and subsequent AE signal are distinguishable. Accurately pinpointing the transition between these phases proves more challenging. The application of traditional machine learning metrics may be influenced by the presence of clearly discernible initial and terminal samples, which may limit the ability to gain insight into the proximity of the expected onset time to the actual onset time. To provide a comprehensive evaluation, the time difference between the predicted and actual onset times was considered. This metric offers more meaningful insights into the models performance. Given the rapid propagation speed of AE signals, it is imperative to minimise the discrepancy between the expected and actual onset times. Even a small error in onset time identification can significantly affect the accuracy of crack location. Table III presents the mean absolute time difference between predicted and actual onset times for all the evaluated neural networks.

The corrective strategy applied to model results considerably increases the methodology precision. The optimal model exhibits an average error of $7\mu s$, which is equivalent to $2.8cm$ positional inaccuracy when the acoustic wave velocity is assumed to be $4000m/s$. This improvement can be attributed to a reduction in false positive onset time events. Figure 4 depicts a comparative analysis of all trained models, which reveals discrepancies in the estimated time delay (Δt) obtained through the proposed methodology. The results indicate that the depth of the U-Nets has a significant influence on the outcomes, with deeper networks resulting in higher accuracy in determining the onset time. The duration of the input signal sequence has a comparatively less pronounced impact on the results. No preprocessing of the data was employed in order to achieve the high accuracy, and the integration of several signals from piezoelectric sensors was not investigated as a potential source of improvement in this study. Although this was not within the scope of the project, which aimed to develop a deep learning strategy for real-time onset time recognition in continuous data, these techniques offer the potential for future

method accuracy improvements.

III. APPLICATION AND RESULTS

This section presents the results obtained by our method on a dataset of authentic acoustic emission signals, without any re-training or finetuning. The signals have been recorded during laboratory investigations of concrete samples, specifically during a three-point bending test on a specimen of fibre-reinforced concrete. The test sample, of size $120 \times 30 \times 15$ cm, exhibited a 5 cm deep notch in the centre. The loading was applied until failure, with control over crack mouth opening displacement (CMOD). A piezoelectric sensor was positioned on the shorter side of the specimen to collect the acoustic emission waveforms generated during the fracture development process. The signals were sampled at a frequency of 1000 kHz. At this stage, the model was tested considering a single signal. Under operational conditions, it will be necessary to use at least 5 sensors simultaneously to perform crack location.

Figure 5 illustrates the effectiveness of the method in distinguishing the AE signals from the background noise. It is acknowledged that the PLB test signals exhibit inherent variations when compared to those generated during the actual crack formation process. Nevertheless, the U-Net model, which was trained exclusively on PLB test signals, has demonstrated a commendable ability to identify acoustic emission signals. It is pertinent to highlight that the aforementioned procedure was tested on signal segments that had been trimmed to align with the length of those utilised for training. It is recommended that model training with real acoustic emission data be conducted in order to achieve greater accuracy and the ability to incorporate continuous signals. It is also important to recognise that the acoustic emission signals tested were acquired in a laboratory setting, which may have resulted in a lower background noise level compared to field-recorded data.

IV. CONCLUSIONS

The study presents a deep learning method for real-time identification of onset times in acoustic emission signals, which is particularly relevant for structural health monitoring (SHM). Experiments on simulated and real data demonstrate the effectiveness of the method in accurately classifying signal samples and distinguishing between background noise and AE signals. The models achieve high levels of accuracy across various evaluation metrics, with minimal mean absolute error (MAE) and a rolling average correction technique significantly improving precision. Future enhancements may involve training the neural network on a diverse dataset of real AE signals to simulate real-world monitoring conditions and improve resilience. This research contributes valuable insights into deep learning for AE signal analysis, advancing SHM practices and enabling innovative solutions for structural defect detection and maintenance management.

ACKNOWLEDGMENTS

This research was supported by project MSCA-RISE-2020 Marie Skłodowska - Curie Research and Innovation Staff

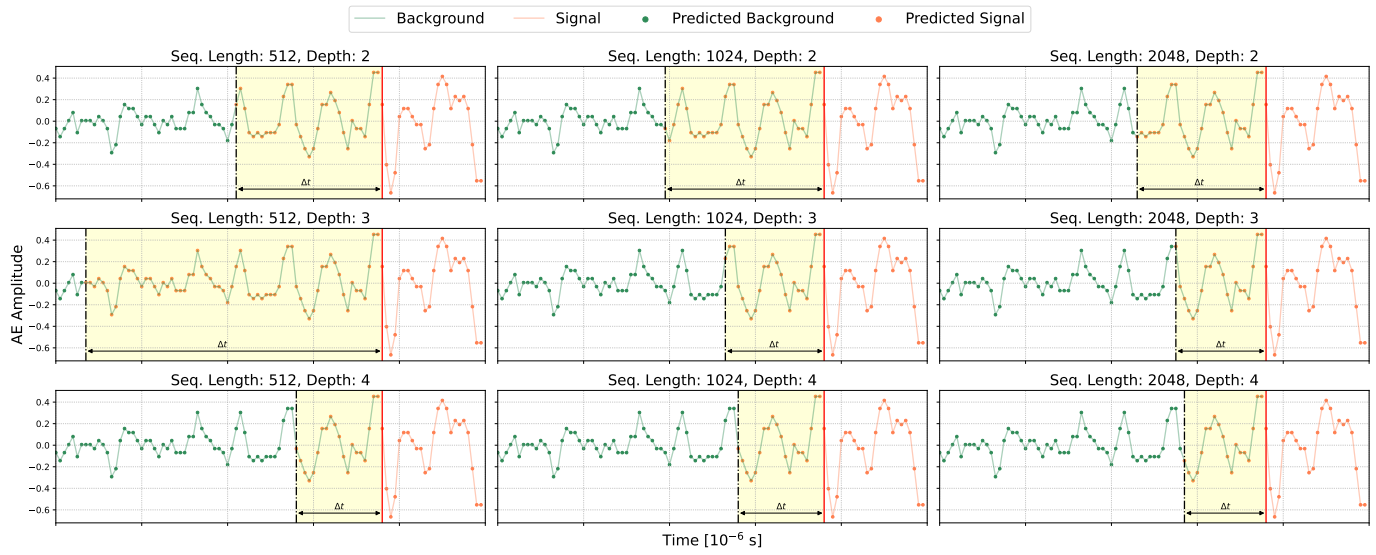


Fig. 4. Comparison of various U-Net models taking into account the difference between the ground truth and the expected onset time.

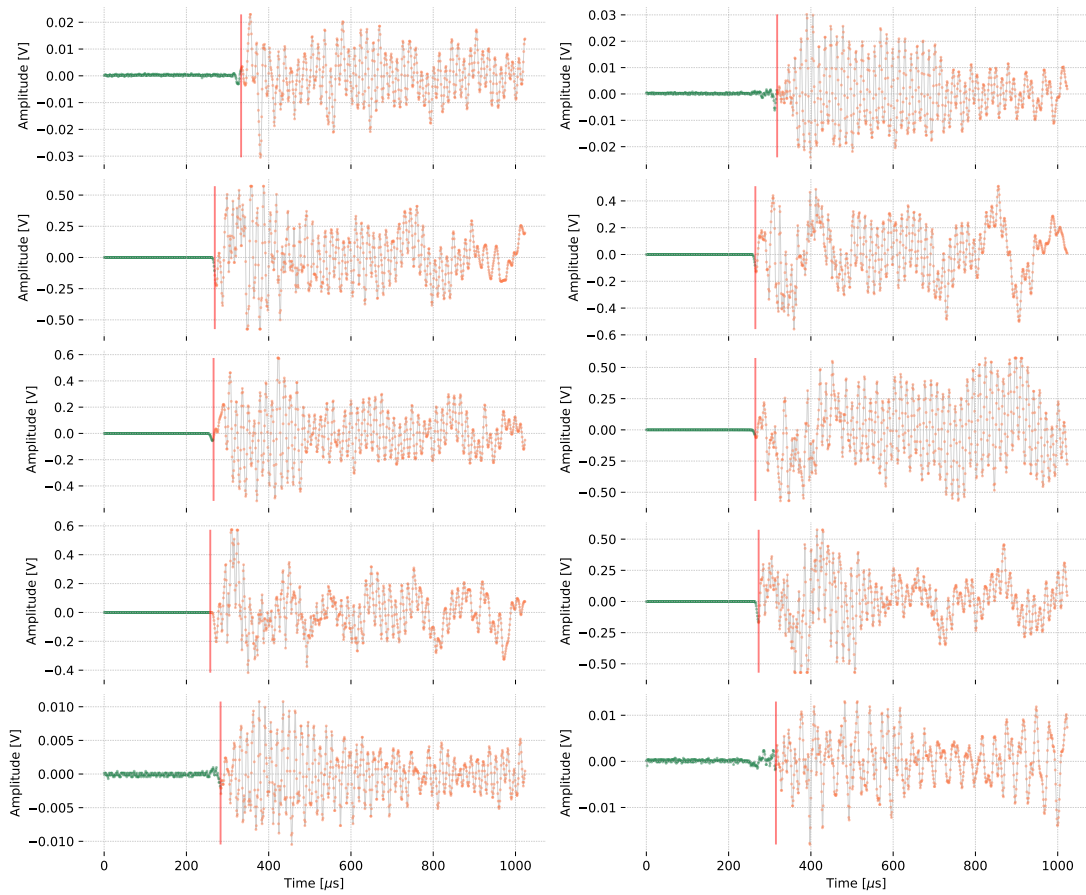


Fig. 5. Validation of the model on real AE signals recorded during a three-point bending test on a fiber-reinforced concrete beam.

| Model | | Train | | | | | | Validation | | | | | |
|-----------|-------|-------|-------|-------|-------|-------|-------|------------|-------|-------|-------|-------|-------|
| Seq. Len. | Depth | Loss | Acc | MAE | RMSE | F1 | AUC | Loss | Acc | MAE | RMSE | F1 | AUC |
| 2048 | 4 | 0.006 | 1.000 | 0.006 | 0.007 | 1.000 | 1.000 | 0.037 | 0.992 | 0.014 | 0.084 | 0.995 | 0.997 |
| 2048 | 3 | 0.010 | 1.000 | 0.010 | 0.013 | 1.000 | 1.000 | 0.065 | 0.985 | 0.026 | 0.115 | 0.990 | 0.991 |
| 2048 | 2 | 0.031 | 0.997 | 0.028 | 0.056 | 0.997 | 1.000 | 0.108 | 0.973 | 0.052 | 0.153 | 0.980 | 0.986 |
| 1024 | 4 | 0.004 | 1.000 | 0.004 | 0.005 | 1.000 | 1.000 | 0.031 | 0.994 | 0.011 | 0.072 | 0.996 | 0.998 |
| 1024 | 3 | 0.007 | 1.000 | 0.007 | 0.010 | 1.000 | 1.000 | 0.061 | 0.986 | 0.021 | 0.109 | 0.991 | 0.991 |
| 1024 | 2 | 0.055 | 0.991 | 0.047 | 0.096 | 0.991 | 0.999 | 0.103 | 0.972 | 0.062 | 0.151 | 0.978 | 0.990 |
| 512 | 4 | 0.012 | 0.999 | 0.008 | 0.019 | 1.000 | 1.000 | 0.032 | 0.993 | 0.015 | 0.072 | 0.996 | 0.998 |
| 512 | 3 | 0.008 | 1.000 | 0.007 | 0.013 | 1.000 | 1.000 | 0.059 | 0.985 | 0.023 | 0.112 | 0.990 | 0.993 |
| 512 | 2 | 0.052 | 0.987 | 0.040 | 0.095 | 0.990 | 0.999 | 0.092 | 0.971 | 0.054 | 0.148 | 0.978 | 0.993 |

TABLE II
MACHINE LEARNING METRICS FOR THE VARIOUS U-NET MODELS.

| Model | Seq. Len. | 2048 | 2048 | 2048 | 1024 | 1024 | 1024 | 512 | 512 | 512 |
|-------------------|-----------------|-------|-------|--------|-------|-------|--------|-------|-------|--------|
| | Depth | 4 | 3 | 2 | 4 | 3 | 2 | 4 | 3 | 2 |
| U-Net predictions | Train | 0 | 0 | 142.83 | 0 | 0 | 211.24 | 5.46 | 0.11 | 242.55 |
| | Validation | 14.63 | 86.27 | 201.98 | 25.58 | 81.71 | 207.67 | 33.53 | 89.39 | 210.33 |
| R.A. corrections | Train | 0 | 0 | 4.74 | 0 | 0 | 19.59 | 3.39 | 0.11 | 25.37 |
| | Validation | 7.03 | 21.34 | 28.56 | 10.62 | 22.12 | 35.64 | 9.01 | 16.51 | 36.02 |
| | Δx (cm) | 2.812 | 8.536 | 11.424 | 4.248 | 8.848 | 14.256 | 3.604 | 6.604 | 14.408 |

TABLE III
AVERAGE TEMPORAL DISTANCE (10^{-6} SECONDS) BETWEEN PREDICTED AND ACTUAL ONSET TIMES, WITH THE CORRESPONDING ESTIMATED POSITIONAL ERROR.

Exchange (RISE) - <http://adoptml.ntua.gr/> - "ADDitively Manufactured OPTimized Structures by means of Machine Learning" (No: 101007595)

REFERENCES

- [1] W. Wang and K. Siau, "Artificial intelligence, machine learning, automation, robotics, future of work and future of humanity: A review and research agenda," *Journal of Database Management (JDM)*, vol. 30, no. 1, pp. 61–79, 2019.
- [2] A. T. G. Tapeh and M. Naser, "Artificial intelligence, machine learning, and deep learning in structural engineering: a scientometrics review of trends and best practices," *Archives of Computational Methods in Engineering*, vol. 30, no. 1, pp. 115–159, 2023.
- [3] T. M. Mitchell, "Machine learning," 1997.
- [4] C. B. Scruby, "An introduction to acoustic emission," *Journal of Physics E: Scientific Instruments*, vol. 20, no. 8, p. 946, 1987.
- [5] F. Lamonaca, P. F. Sciammarella, C. Scuro, D. L. Carnì, and R. S. Olivito, "Synchronization of iot layers for structural health monitoring," in *2018 Workshop on Metrology for Industry 4.0 and IoT*. IEEE, 2018, pp. 89–94.
- [6] A. Manuello Bertetto, F. Marmo, and J. Melchiorre, "Acoustic emission monitoring and thrust network analysis of the central nave vaults of the turin cathedral," in *Italian Workshop on Shell and Spatial Structures*. Springer, 2023, pp. 241–249.
- [7] A. Manuello, F. Marmo, and J. Melchiorre, "Investigating and monitoring central nave vaults of the turin cathedral with acoustic emissions and thrust network analysis," *Developments in the Built Environment*, vol. 18, p. 100434, 2024.
- [8] G. Lacidogna, A. Manuello, G. Niccolini, and A. Carpinteri, "Acoustic emission monitoring of italian historical buildings and the case study of the athena temple in syracuse," *Architectural Science Review*, vol. 58, no. 4, pp. 290–299, 2015.
- [9] A. Arnau *et al.*, *Piezoelectric transducers and applications*. Springer, 2004, vol. 2004.
- [10] D. G. Aggelis, "Classification of cracking mode in concrete by acoustic emission parameters," *Mechanics Research Communications*, vol. 38, no. 3, pp. 153–157, 2011.
- [11] A. Carpinteri, J. Xu, G. Lacidogna, and A. Manuello, "Reliable onset time determination and source location of acoustic emissions in concrete structures," *Cement and concrete composites*, vol. 34, no. 4, pp. 529–537, 2012.
- [12] F. Bai, D. Gagar, P. Foote, and Y. Zhao, "Comparison of alternatives to amplitude thresholding for onset detection of acoustic emission signals," *Mechanical Systems and Signal Processing*, vol. 84, pp. 717–730, 2017.
- [13] J. H. Kurz, C. U. Grosse, and H.-W. Reinhardt, "Strategies for reliable automatic onset time picking of acoustic emissions and of ultrasound signals in concrete," *Ultrasonics*, vol. 43, no. 7, pp. 538–546, 2005.
- [14] J. Melchiorre, A. Manuello Bertetto, M. M. Rosso, and G. C. Marano, "Acoustic emission and artificial intelligence procedure for crack source localization," *Sensors*, vol. 23, no. 2, p. 693, 2023.
- [15] P.-H. Chen, J.-J. Ding, J.-Y. Huang, and T.-Y. Tseng, "Accurate onset detection algorithm using feature-layer-based deep learning architecture," in *2020 IEEE International Symposium on Circuits and Systems (ISCAS)*. IEEE, 2020, pp. 1–5.
- [16] F. Zonzini, D. Bogomolov, T. Dhamija, N. Testoni, L. De Marchi, and A. Marzani, "Deep learning approaches for robust time of arrival estimation in acoustic emission monitoring," *Sensors*, vol. 22, no. 3, p. 1091, 2022.
- [17] J. Melchiorre, L. D'Amato, F. Agostini, and A. M. Rizzo, "Acoustic emission onset time detection for structural monitoring with u-net neural network architecture," *Developments in the Built Environment*, p. 100449, 2024.
- [18] M. Zhang, M. Li, J. Zhang, L. Liu, and H. Li, "Onset detection of ultrasonic signals for the testing of concrete foundation piles by coupled continuous wavelet transform and machine learning algorithms," *Advanced Engineering Informatics*, vol. 43, p. 101034, 2020.
- [19] J. Melchiorre, M. M. Rosso, R. Cucuzza, E. D'Alto, A. Manuello, and G. C. Marano, "Deep acoustic emission detection trained on seismic signals," in *Applications of Artificial Intelligence and Neural Systems to Data Science*. Springer, 2023, pp. 83–92.
- [20] O. Ronneberger, P. Fischer, and T. Brox, "U-net: Convolutional networks for biomedical image segmentation," in *Medical Image Computing and Computer-Assisted Intervention – MICCAI 2015*, N. Navab, J. Hornegger, W. M. Wells, and A. F. Frangi, Eds. Cham: Springer International Publishing, 2015, pp. 234–241.
- [21] R. Madarshahian, V. Soltangharai, R. Anay, J. M. Caicedo, and P. Ziehl, "Hsu-nielsen source acoustic emission data on a concrete block," *Data in Brief*, vol. 23, p. 103813, 2019. [Online]. Available: <https://www.sciencedirect.com/science/article/pii/S2352340919301647>
- [22] F. Lamonaca, A. Carrozzi, D. Grimaldi, and R. S. Olivito, "Improved monitoring of acoustic emissions in concrete structures by multi-triggering and adaptive acquisition time interval," *Measurement*, vol. 59, pp. 227–236, 2015.